New Virial-Type Model for Predicting Single- and Multicomponent Isosteric Heats of Adsorption

ARTICLE *in* INDUSTRIAL & ENGINEERING CHEMISTRY RESEARCH · FEBRUARY 1998

Impact Factor: 2.59 · DOI: 10.1021/ie970577y

2 AUTHORS, INCLUDING:

Shaheen Abdulhafez Al-Muhtaseb
Qatar University
60 PUBLICATIONS **769** CITATIONS

SEE PROFILE

New Virial-Type Model for Predicting Single- and Multicomponent Isosteric Heats of Adsorption

Shaheen A. Al-Muhtaseb and James A. Ritter*

Department of Chemical Engineering, Swearingen Engineering Center, University of South Carolina, Columbia, South Carolina 29208

The virial isotherm for single- and multicomponent gas adsorption equilibria was used to derive a new predictive model for the isosteric heat of adsorption. The virial coefficients were considered with two different orders of temperature dependencies. The coefficients with a first-order dependence of the temperature reciprocal showed that the single-component isosteric heat of adsorption is temperature independent. However, those with second-order dependence of the temperature reciprocal showed that the single-component isosteric heat of adsorption can vary significantly with temperature. The latter form also showed when lateral or vertical interactions dominated. Both types of coefficients showed a significant temperature dependence of the multicomponent isosteric heat of adsorption. Differences between single- and multicomponent isosteric heats of adsorption, compared at the same temperature and partial loading, also increased with decreasing adsorbed phase mole fraction, decreasing temperature, higher adsorption affinity, and increasing nonideality.

Introduction

Adsorption is generally known to be an exothermic processes. Therefore, the design of adsorption processes requires accurate predictions of the thermal properties of single- and multicomponent gas adsorption equilibria. The classical technique for predicting the isosteric heat of adsorption depends on fitting single component adsorption isotherms to a loading-explicit isotherm model, using the chain rule to convert the temperature derivative of pressure at constant loading to temperature and pressure derivatives of loading, and performing numerical differentiation (Sircar, 1991a; Sircar, 1992). However, this multistep process cannot be practically applied to more than binary mixtures because the use of the chain rule for multicomponent adsorption equilibria leaves numerous derivatives to be determined numerically.

Direct methods for measuring the isosteric heat of adsorption are available and based on dosing calorimetry (O'Neil *et al.*, 1985; Parillo and Gorte, 1992; Handy *et al.*, 1993; Dunne *et al.*, 1996a; Dunne *et al.*, 1996b; Dunne *et al.*, 1997). But, most of these techniques are for single components, with only one very recent technique for multicomponents (Dunne *et al.*, 1997). These calorimeters are also not readily available, although much information has been published on how to construct such an apparatus (O'Neil *et al.*, 1985; Parillo and Gorte, 1992; Handy *et al.*, 1993). Molecular models are also being explored for prediction of the isosteric heat of adsorption. These studies, however, are still in their infancy, because fairly simple model systems are being explored with very few results being compared with experiment or the classical technique. Notable exceptions include the molecular simulations carried out by Karavias and Myers (1991) and the density functional theory study by Pan *et al.* (1997). Clearly, what is needed is a temperature-dependent, pressure-explicit isotherm model for single- and mixed-gas adsorption that leads to explicit expressions for single- and multicomponent isosteric heats of adsorption.

Several models are available in the literature that describe the temperature dependence of gas adsorption equilibria. Most of these models depend on the Polanyi pore-filling concept to obtain an explicit temperature dependence (Dubinin, 1989; Bering *et al.*, 1963; Polanyi, 1932). Other models, such as the extended Langmuir (EL) model and the analytical heterogeneous extended Langmuir (AHEL), were also used to successfully describe the temperature dependence of adsorption equilibria (Kapoor *et al.*, 1990). However, such loading-explicit models are not very promising for the prediction of the isosteric heat of adsorption. Even those isotherms that can be manipulated as pressure-explicit isotherms (e.g., the EL and the AHEL isotherms) are known to loose much of their accuracy after such manipulation.

Instead, other pressure-explicit models, such as the modified Antoine isotherm (Hacskaylo and LeVan, 1985) and the virial adsorption isotherm (Haydel and Kobayashi, 1967; Barrer and Davies, 1970; Pierotti and Thomas, 1974; Czepirski and Jagiello, 1989; Zhang *et al.*, 1991; DeGance, 1992; DeGance *et al.*, 1993; Taqvi and LeVan, 1997a; Taqvi and LeVan, 1997b), can be more usefully applied to predict the isosteric heat of adsorption because they are based solely on pressure-explicit correlations in terms of temperature and loading. The virial description of multicomponent adsorption equilibria is seemingly very powerful because it accounts for the different types of nonidealities and interactions within the adsorbed phase. For example, the expanded virial equations for mixtures (Taqvi and LeVan, 1997b) account for different degrees of adsorbate−adsorbate interactions with every additional virial coefficient. Thus, the second virial coefficient describes interactions between each pair of molecules, the third virial coefficient describes interactions among every triplet of molecules, and so on. However, only Czepiriski and Jagiello (1989) developed an expression for predicting single-component isosteric heats of adsorption, and essentially no work has been done on predicting mul-

* To whom all correspondence should be addressed. Phone: (803) 777-3590. Fax: (803) 777-8265. E-mail: ritter@sun.che.sc.edu.

S0888-5885(97)00577-0 CCC: $15.00
Published on Web 02/02/1998

ticomponent heats of adsorption from virial type expressions or otherwise.

In this work, the single-component virial isotherm (Czepiriski and Jagiello, 1989; Taqvi and LeVan, 1997a) and its extension to multicomponent systems (Taqvi and LeVan, 1997b) are adopted to predict the isosteric heats of adsorption of single and multicomponent gas adsorption equilibria. This completely analytic extension adequately describes the nonidealities of the systems and distinguishes between adsorbate−adsorbate and adsorbate−adsorbent interactions. The temperature dependence of the virial coefficients is also studied.

Theory

The virial adsorption isotherm that has been used to describe single-component gas adsorption (Czepirski and Jagiello, 1989; Taqvi and LeVan, 1997a) is expressed as follows:

$$\ln\left(\frac{P}{Q}\right) = A + \frac{2}{a}BQ + \frac{3}{2a^2}CQ^2 + \dots \tag{1}$$

The statistical mechanics show that the second virial coefficient, B, reflects interactions between pairs of molecules, the third virial coefficient, C, reflects interactions between triples of molecules, ... etc. For most systems, the virial equation can be safely truncated after the third virial coefficient. However, the virial equation can sometimes diverge for very high gas concentrations. The temperature dependence of the virial coefficients is described by eq 2:

$$A = \sum_{m=0}^{\infty}\frac{A^{(m)}}{T^m}, \qquad B = \sum_{m=0}^{\infty}\frac{B^{(m)}}{T^m}, \qquad C = \sum_{m=0}^{\infty}\frac{C^{(m)}}{T^m}, \qquad \dots \tag{2}$$

which can be truncated after the second or third term. Different forms of temperature dependence have been examined by several investigators (Barrer and Davies, 1970; Zhang *et al.*, 1991; Taqvi and LeVan, 1997a), and the most representative behavior was expressed in terms of the temperature reciprocal.

Taqvi and LeVan (1997b) further extended the virial isotherm to multicomponent adsorption equilibria. They proposed extended virial coefficients according to mixing rules that satisfy the adsorbate−adsorbate interactions in both predictive and correlative modes. This extended isotherm is expressed in its predictive mode for a homogeneous adsorbent as follows:

$$\ln\left(\frac{P_i}{Q_i}\right) = A_i + \left(\frac{2}{a}\right)\sum_{j=1}^{N}B_{ij}Q_j + \left(\frac{3}{2a^2}\right)\sum_{j=1}^{N}\sum_{k=1}^{N}C_{ijk}Q_jQ_k + \dots \tag{3}$$

where

$$B_{ij} = \frac{1}{4}(\sqrt{B_{ii}} + \sqrt{B_{jj}})^2, \qquad B_{ii} = B_i \tag{4}$$

$$C_{ij} = \frac{1}{16}(C_{iii}^{1/4} + C_{jjj}^{1/4})^4, \qquad C_{iii} = C_i \tag{5}$$

$$C_{ijk} = (C_{ij}C_{jk}C_{ik})^{1/3} \tag{6}$$

The isosteric heat of adsorption is described by the Clausius−Clapeyron equation for both single- and mixed-gas adsorption, as shown in eqs 7 and 8, respectively (Sircar, 1991a; Sircar, 1992).

$$q = RT^2\left[\frac{\partial \ln P}{\partial T}\right]_Q \tag{7}$$

$$q_i = RT^2\left[\frac{\partial \ln P_i}{\partial T}\right]_{Q_i} \tag{8}$$

The subscript Q indicates that the amount adsorbed is held constant while taking the derivatives. Previous treatments (Sircar, 1991a; Sircar, 1992) depended on replacing the pressure term in the aforementioned definitions by the amount adsorbed at both constant temperature and pressure using the chain rule. The complexity of the resulting relations dramatically increased with every component added to the mixture. Thus, such a technique is not practical for more than binary mixtures.

Applying the definitions just shown to the virial adsorption isotherms (eqs 1 and 3) results in explicit expressions for the isosteric heats of adsorption for single- and multicomponent gas adsorption. The single-component isosteric heat of adsorption is expressed as shown in eqs 9 and 10 for virial coefficients of the order $O(T^{-1})$ and $O(T^{-2})$, respectively:

$$q^{(1/T)} = \frac{-R}{a^2}\left(a^2A^{(1)} + 2aQB^{(1)} + \frac{3}{2}Q^2C^{(1)}\right) \tag{9}$$

$$q^{(1/T^2)} = \frac{-R}{a^2}\left(a^2A^{(1)} + 2aQB^{(1)} + \frac{3}{2}Q^2C^{(1)} + \left(\frac{1}{T}\right)(2a^2A^{(2)} + 4aQB^{(2)} + 3Q^2C^{(2)})\right) \tag{10}$$

The multicomponent isosteric heat of adsorption is given by:

$$q_i = \frac{RT^2}{a^2}\left(a^2A_i' + 2a\sum_{j=1}^{N}B_{ij}'Q_j + \frac{3}{2}\sum_{j=1}^{N}\sum_{k=1}^{N}C_{ijk}'Q_jQ_k\right) \tag{11}$$

where

$$B_{ij}' = \frac{\partial B_{ij}}{\partial T} = \frac{(\sqrt{B_i} + \sqrt{B_j})(\sqrt{B_j}B_i' + \sqrt{B_i}B_j')}{4\sqrt{B_iB_j}} \tag{12}$$

$$C_{ijk}' = \frac{\partial C_{ijk}}{\partial T} = \frac{1}{48}(X_1X_2X_3)^{1/3}\left(X_1X_2\left(\frac{C_i'}{C_i^{3/4}} + \frac{C_j'}{C_j^{3/4}}\right) + X_1X_3\left(\frac{C_j'}{C_j^{3/4}} + \frac{C_k'}{C_k^{3/4}}\right) + X_2X_3\left(\frac{C_i'}{C_i^{3/4}} + \frac{C_k'}{C_k^{3/4}}\right)\right) \tag{13}$$

and

$$X_1 = C_i^{1/4} + C_k^{1/4} \tag{14}$$

$$X_2 = C_j^{1/4} + C_k^{1/4} \tag{15}$$

$$X_3 = C_i^{1/4} + C_j^{1/4} \tag{16}$$

Equation 11 depends only on the fitted parameters from the single-component form of the virial equation when proper mixing rules are applied. Therefore, the aforementioned relations suggest an alternative technique for the prediction of mixed-gas isosteric heats of adsorption for an unlimited number of components and with-

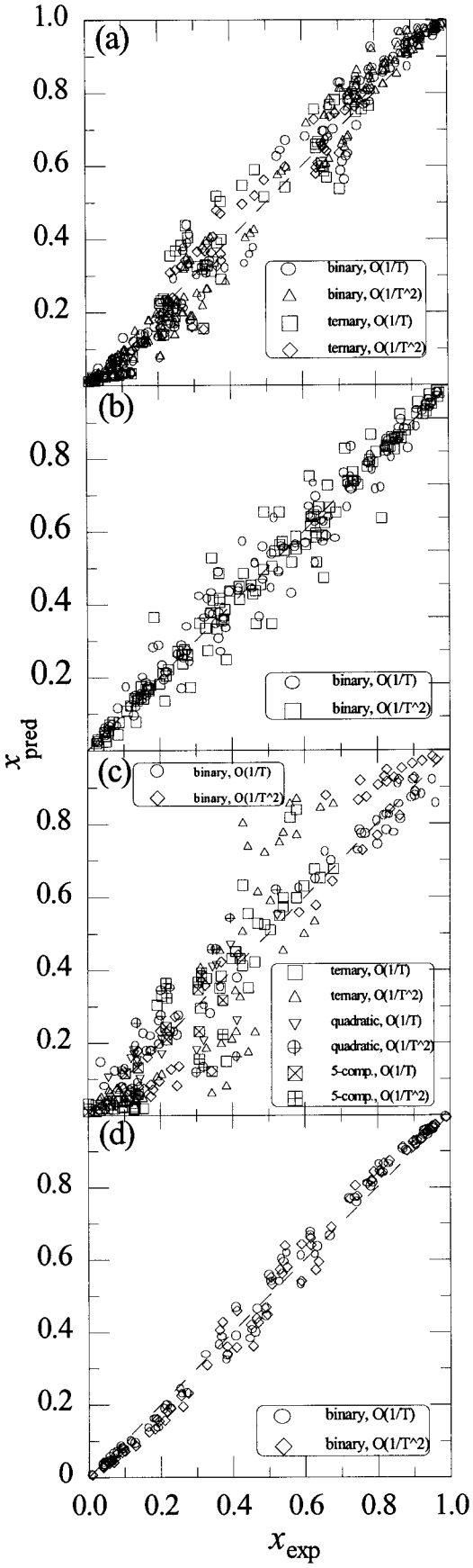

Figure 1. A comparison between the predicted and experimental multicomponent adsorbed phase composition on (a) BPL-activated carbon (Reich *et al.*, 1980), (b) Nuxite-AL-activated carbon (Szepesy and Illes, 1963c), (c) PCB-activated carbon (Ritter and Yang, 1987), and (d) 13X molecular sieve zeolite (Danner and Choi, 1978; Hyun and Danner, 1982; Kaul, 1987).

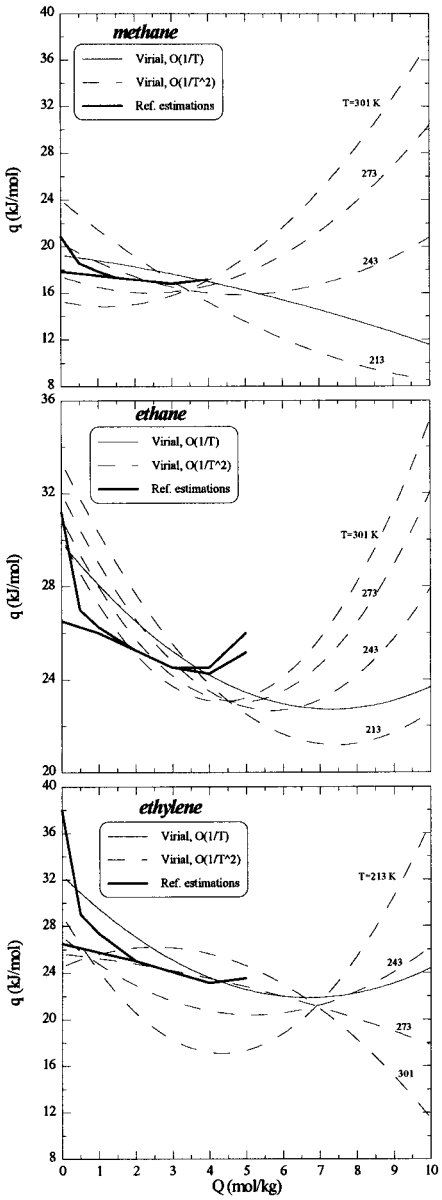

Figure 2. Single-component isosteric heats of adsorption on BPL-activated carbon (Reich *et al.*, 1980) using the virial adsorption isotherm with parameters $O(T^{-1})$ (solid thin line) and $O(T^{-2})$ (dashed lines) compared with literature estimations (solid thick lines; Valenzuela and Myers, 1989).

out complicating the equations or adding any further source of uncertainty, such as replacing one derivative by two or more derivatives when using the chain rule. Moreover, eq 11 meets two thermodynamic consistency criteria. The first criterion recommended by Dunne *et al.* (1997) for binary mixtures is

$$\left(\frac{\partial q_1}{\partial Q_2}\right)_{T,Q_1} = \left(\frac{\partial q_2}{\partial Q_1}\right)_{T,Q_2} \tag{17}$$

Applying eq 11 to eq 17 leads to

$$\left(\frac{\partial q_1}{\partial Q_2}\right)_{T,Q_1} = \left(\frac{\partial q_2}{\partial Q_1}\right)_{T,Q_2} = \frac{RT^2}{a^2}(2aB'_{12} + 3C'_{112}Q_1 + 3C'_{122}Q_2) \tag{18}$$

The second criterion recommended by Dunne *et al.* (1997) is

Table 1. Single-Component Isotherm Data Sets Fitted to the Virial Adsorption Isotherm

adsorbent	$10^{-3} \times a$ (m^3/kg)	adsorbate	temp. range (K)	ref[b]	$ARE^{O(1/T)}$ (%)	$ARE^{O(1/T2)}$ (%)
BPL-activated carbon	988	ethane	213−301	RZR	12.10	11.29
		ethylene	213−301	RZR	6.29	10.41
		methane	213−301	RZR	5.81	4.11
Nuxite-AL-activated carbon	950[a]	butane	293−363	SI1	39.06	39.96
		carbon dioxide	293−363	SI1, SI2	16.08	13.02
		ethane	293−363	SI1, SI2	7.38	7.13
		ethylene	293−363	SI1, SI2	6.17	6.98
		methane	293−363	SI1, SI2	3.12	3.09
		propane	293−363	SI1, SI2	17.05	12.95
		propylene	293−363	SI1, SI2	18.69	18.07
PCB-activated carbon	950[a]	carbon dioxide	296−480	RY	14.40	10.11
		carbon monoxide	296−473	RY	3.35	3.06
		hydrogen	296−480	RY	9.64	5.95
		hydrogen sulfide	296−480	RY	7.07	8.15
		methane	296−480	RY	15.87	9.80
13X molecular sieve zeolite	525	ethane	273−423	DC, HD, K	16.50	16.72
		ethylene	298−423	DC, HD, K	17.59	17.65

[a] These values were assumed because insufficient information was provided. [b] DC = Danner and Choi (1978); HD = Hyun and Danner (1982); K = Kaul (1987); RY = Ritter and Yang (1987); RZR = Reich *et al.* (1980); SI1 = Szepesy and Illes (1963 a); SI2 = Szepesy and Illes (1963 b).

Table 2. Adsorption Virial Coefficients $O(T^{-1})$

adsorbent	adsorbate	$A^{(0)}$	$A^{(1)}$ (K)	$B^{(0)}$ (kg·m²/mol)	$10^{-7} \times B^{(1)}$ (kg·m²·K/mol)	$10^{-10} \times C^{(0)}$ (kg²·m⁴/mol²)	$10^{-13} \times C^{(1)}$ (kg²·m⁴·K/mol²)
BPL-activated carbon	methane	14.414	−2317	119 907	2.624	−0.687	0.259
	ethane	15.268	−3596	−52 442	11.663	4.948	−1.049
	ethylene	17.588	−3891	−445 472	18.576	8.602	−1.824
Nuxite-AL-activated carbon	methane	13.017	−1926	1 749 018	−44.838	−10.810	32.105
	ethylene	15.824	−3525	6317	7.476	1.643	−0.227
	ethane	15.809	−3611	−63 847	9.057	1.691	0.000
	propylene	13.808	−3628	202 860	0.000	6.544	0.000
	propane	23.215	−6601	−1 398 338	47.283	24.342	−4.487
	butane	26.375	−9910	−922 919	71.828	+0.000	0.000
	CO_2	15.837	−3130	7.024	4.442	2×10^{-4}	0.000
PCB-activated carbon	methane	15.391	−3222	213 839	4.791	1×10^{-4}	0.000
	CO	12.776	−1591	426 863	−12.307	−0.681	1.420
	CO_2	15.616	−3462	97 484	3.458	6×10^{-5}	0.000
	H_2	15.759	−1756	−576 968	21.395	2×10^{-7}	0.000
	H_2S	12.781	−2481	289 969	−8.467	−2.641	1.256
13X molecular sieve zeolite	ethane	16.154	−3573	207 945	−6.196	6×10^{-5}	1.943
	ethylene	18.894	−5262	548	2.498	−3.932	3.727

Table 3. Adsorption Virial Coefficients $O(T^{-2})$

adsorbent	adsorbate	$A^{(0)}$	$A^{(1)}$ (K)	$10^{-5} \times A^{(2)}$ (K^2)	$B^{(0)}$ (kg·m²/mol)	$10^{-8} \times B^{(1)}$ (kg·m²·K/mol)	$10^{-10} \times B^{(2)}$ (kg·m²·K²/mol)	$10^{-11} \times C^{(0)}$ (kg²·m⁴/mol²)	$10^{-13} \times C^{(1)}$ (kg²·m⁴·K/mol²)	$10^{-15} \times C^{(2)}$ (kg²·m⁴·K²/mol²)
BPL-activated carbon	methane	9.099	694	−3.813	365 905	−2.282	4.092	1.669	−5.902	5.390
	ethane	14.376	−2679	−1.421	−436 892	1.943	1×10^{-6}	1.804	−5.955	4.514
	ethylene	12.153	−1664	−1.935	2 085 408	−10.517	14.644	−3.272	18.873	−25.306
Nuxite-AL-activated carbon	methane	13.063	−1938	0.000	1 501 286	−3.276	−1.416	−5.199	−0.266	46.666
	ethylene	14.406	−3037	0.002	348 092	−0.437	0.000	0.395	−3.094	7.284
	ethane	−2.515	7953	−18.095	2 306 616	−12.397	19.836	−0.914	3.470	1×10^{-5}
	propylene	53.414	−2 7325	34.956	68 628	0.000	0.000	−24.999	164.543	−258.268
	propane	9.358	2006	−13.944	−139 051	0.000	3.714	−0.087	2.837	−0.012
	butane	−10.706	20 528	−54.776	−2082	−12.009	37.643	2.844	0.000	0.000
	CO_2	40.300	−19 729	27.820	−4 539 643	31.118	−51.159	1×10^{-6}	0.000	0.000
PCB-activated carbon	methane	3.451	6556	−18.315	998 641	−5.896	8.712	−0.536	4.013	0.000
	CO	13.002	−1782	0.329	311 842	0.000	−2.614	−0.490	2.685	0.000
	CO_2	8.361	2101	−9.665	188 428	0.258	−2.337	0.000	−1.340	6.226
	H_2	18.298	−3948	4.411	140 544	−0.146	0.000	3×10^{-7}	0.000	0.000
	H_2S	12.987	−2590	0.000	133 735	0.543	−2.691	−0.427	1.676	0.211
13X M. S. molecular	ethane	11.481	27	−6.733	306	0.004	-3×10^{-4}	2.867	−15.966	28.378
	ethylene	−3.180	10 721	−28.370	2 836 529	−19.978	34.940	3×10^{-4}	1.640	4.107

$$\lim_{x_i \to 1} q_i = q_i^0 \qquad (19)$$

It is easy to show that eq 11 leads to eq 10 upon applying eq 19. This last criterion is also proven below with actual results.

Results and Discussion

Single-Component Correlation and Multicomponent Prediction of Adsorption Equilibria. Single-component adsorption isotherm systems were selected to cover a variety of adsorbates (hydrogen, methane, ethane, ethylene, propane, propylene, butane, carbon monoxide, carbon dioxide, and hydrogen sulfide) over four different adsorbents: (a) BPL-activated carbon, (b) Nuxite-AL-activated carbon, (c) PCB-activated carbon, and (d) 13X molecular sieve zeolite. A brief compilation of these data is shown in Table 1. The virial coefficients were fitted to these data by the least sum squared error technique (LSSE) in predicting the equilibrium pressure for each adsorbent−adsorbate combination. The fit was

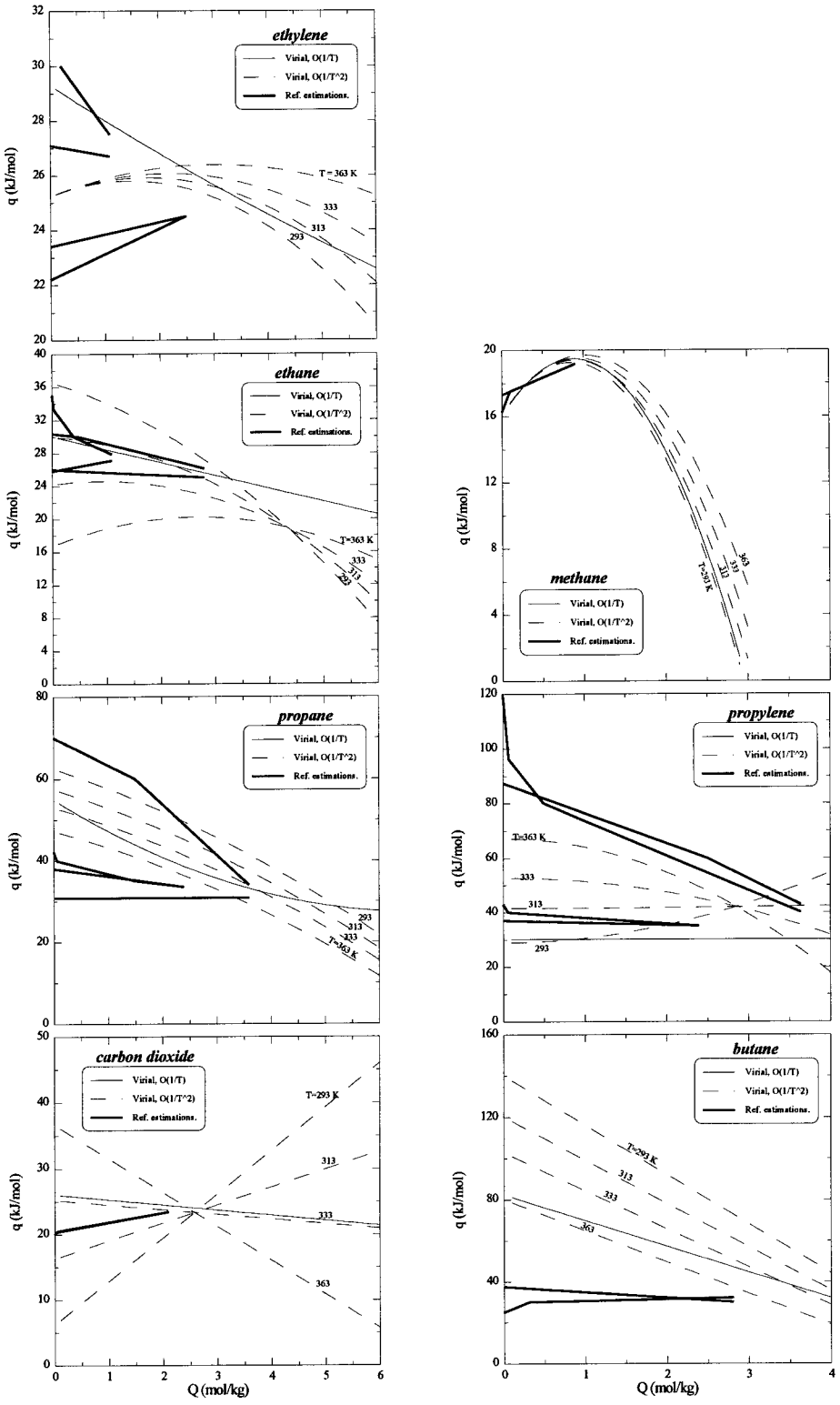

Figure 3. Single-component isosteric heats of adsorption on Nuxite-AL-activated carbon (Szepesy and Illes, 1963a; Szepesy and Illes, 1963b) using the virial adsorption isotherm with parameters O(T^{-1}) (solid thin line) and O(T^{-2}) (dashed lines) compared with literature estimations (solid thick lines; Valenzuela and Myers, 1989).

measured in terms of the absolute relative error (ARE), which is defined as:

$$\mathrm{ARE} = \frac{(100\%)}{n}\sum_{i=1}^{n}\left[\frac{|P^{\mathrm{exp}} - P^{\mathrm{calc}}|}{P^{\mathrm{exp}}}\right]_i \qquad (20)$$

Table 1 shows that the ARE values of the correlated single-component adsorption isotherms were quite satisfactory when considering that the measure of the fit was in terms of the equilibrium pressure. The correlations were noticeably more accurate, however, for the lightly adsorbed components. The corresponding virial coefficients for these data sets are shown in Tables 2 and 3 for O(T^{-1}) and O(T^{-2}), respectively. As a general trend, the temperature dependence decreased with every additional virial coefficient (i.e., the temperature

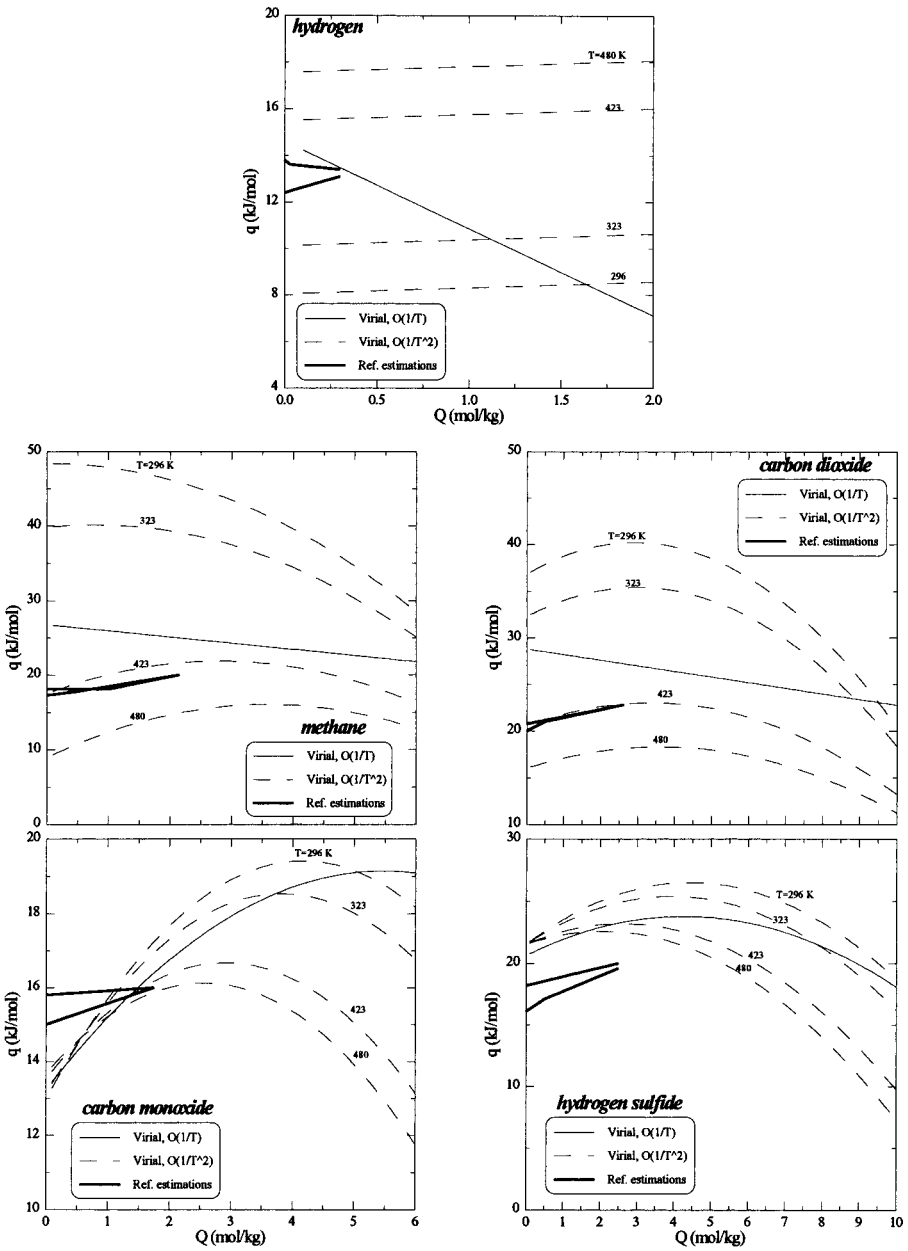

Figure 4. Single-component isosteric heats of adsorption on PCB-activated carbon (Ritter and Yang, 1987) using the virial adsorption isotherm with parameters $O(T^{-1})$ (solid thin line) and $O(T^{-2})$ (dashed lines) compared with literature estimations (solid thick lines; Valenzuela and Myers, 1989).

dependence of the first virial coefficient was higher than that of the second virial coefficient and so on).

The multicomponent adsorption equilibrium data were predicted by solving eqs 3−6 simultaneously for the amount adsorbed of each component using only the parameters fitted to the single-component isotherms. The absolute differences between the left- and right-hand sides of the resulting nonlinear system of equations (eq 3 applied to each component in the mixture) were minimized simultaneously using a Microsoft Excel 7.0a optimizer with a Newton search method, central derivatives, quadratic estimates, automatic scaling, precision of 10^{-5}, and tolerance of 5%. Figure 1 shows the predicted and experimental multicomponent adsorbed phase compositions at the experimental partial pressure of each component in the mixture. The predictions were quite satisfactory considering the various sources of errors that can be associated with the multicomponent experimental data points themselves.

Single-Component Isosteric Heats of Adsorption. Figures 2−5 show the predicted isosteric heats of adsorption from the fitted single-component adsorption isotherms. The same data were also used by Valenzuela and Myers (1989) to estimate the isosteric heats of adsorption of these components by applying the classical chain rule technique to the Toth and UNILAN isotherms. Their estimates were used as a reference to compare the predictions obtained from the virial relation. Almost all of the predictions of the single-component isosteric heats of adsorption using both types of virial coefficients fell within the same range as the reference estimations. In general, the predictions of the virial equation with $O(T^{-1})$ coefficients were very close to the reference values in the range of their estimations. This result was not surprising because the technique used by Valenzuela and Myers (1989) assumes temperature independence of the isosteric heats of adsorption as do the predictions with $O(T^{-1})$ virial coefficients.

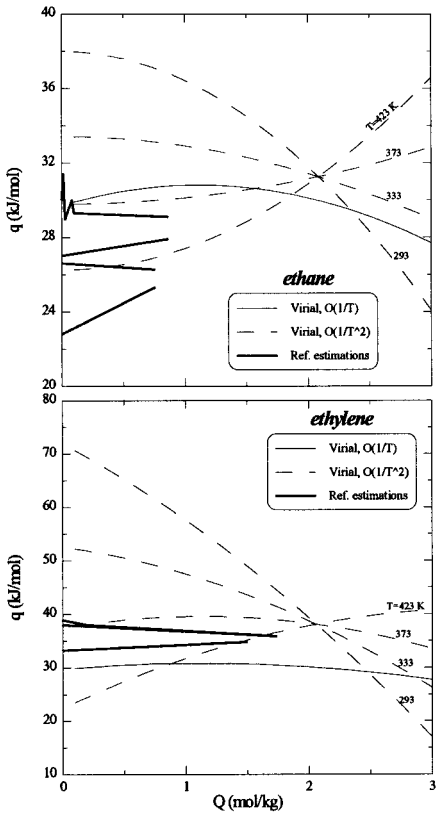

Figure 5. Single-component isosteric heats of adsorption on 13X molecular sieve zeolite (Danner and Choi, 1978; Hyun and Danner, 1982; Kaul, 1987) using the virial adsorption isotherm with parameters $O(T^{-1})$ (solid thin line) and $O(T^{-2})$ (dashed lines) compared with literature estimations (solid thick lines; Valenzuela and Myers, 1989).

Nevertheless, in most cases, the reference values as well as $O(T^{-1})$ estimations were close to the predicted isosteric heats of adsorption at the average temperature when using $O(T^{-2})$ virial coefficients.

According to the predictions from the virial equation with $O(T^{-2})$ coefficients, the single-component isosteric heat of adsorption can sometimes vary significantly with temperature. This variation suggests that the concept blindly adopted by most investigators (i.e., the isosteric heat of adsorption is temperature independent) can only be used as an approximation when dealing with experimental data over relatively narrow ranges of temperature. If wide temperature ranges are to be considered, the temperature dependence, such as that indicated by the virial equation with $O(T^{-2})$ coefficients, should be considered.

Moreover, the predictions of the virial equation exhibited a phenomenon that can be used to indicate the conditions when lateral or vertical interactions dominate. According to eqs 9 and 10, the isosteric heat of adsorption changes in different ways at different conditions. The relative changes of the isosteric heat of adsorption with respect to loading and temperature are given by:

$$\left[\frac{\partial q^{(1/T)}}{\partial Q}\right]_T = \frac{-R}{a^2}(2aB^{(1)} + 3QC^{(1)}) \tag{21}$$

$$\left[\frac{\partial q^{(1/T^2)}}{\partial Q}\right]_T = \frac{-R}{a^2}\left(2aB^{(1)} + 3QC^{(1)} + \frac{4aB^{(2)} + 6QC^{(2)}}{T}\right) \tag{22}$$

$$\left[\frac{\partial q^{(1/T^2)}}{\partial T}\right]_Q = \frac{R}{a^2T^2}(2a^2A^{(2)} + 4aQB^{(2)} + 3Q^2C^{(2)}) \tag{23}$$

Therefore, the estimated single-component isosteric heat of adsorption at constant temperature inverts at some loading when either lateral or vertical interactions dominate. This optimum loading is shown in eqs 24 and 25 as estimated from the first- and second-order temperature dependencies of eqs 21 and 22, respectively.

$$Q_{opt}^{(1/T)}|_T = \frac{-2a}{3}\left(\frac{B^{(1)}}{C^{(1)}}\right) \tag{24}$$

$$Q_{opt}^{(1/T^2)}|_T = \frac{-2a}{3}\left(\frac{B^{(1)}T + 2B^{(2)}}{C^{(1)}T + 2C^{(2)}}\right) \tag{25}$$

This result indicates that inversion can occur only at a specific ratio of molecular interactions between pairs and triplets of molecules (ratio between B and C coefficients), and supports the potential capability of the derived model to indicate when different interactions change with loading, as indicated by changes in the isosteric heat of adsorption (Sircar, 1991b). This feature adds another advantage of the virial-based predictions of the isosteric heat of adsorption, especially when the $O(T^{-2})$ coefficients are used. In addition, eq 23 indicates that at a fixed Q, temperature cannot cause an inversion; but if Q is allowed to change, then temperature can participate in the inversion, as indicated in eq 22, which approaches zero when

$$T_{opt} = -2\frac{2aB^{(2)} + 3QC^{(2)}}{2aB^{(1)} + 3QC^{(1)}} \tag{26}$$

At constant loading, the temperature variation can only change the relative dependence of the isosteric heat of adsorption on this loading. However, the sign of this change inverts only at specific loadings when the temperature effect is overcome with the opposing lateral and vertical interactions. These loadings are obtained by setting eq 23 to zero, which gives

$$Q_{opt}^{(1/T^2)}|_Q = \frac{a}{3C^{(2)}}(-2B^{(2)} \pm \sqrt{4(B^{(2)})^2 - 6A^{(2)}C^{(2)}}) \tag{27}$$

Therefore, the second-order virial equation predicts that there are two possible intersections of the isosteric heats of adsorption estimated at different temperatures, as indicated in eq 27. These intersections are generally observed in Figures 2, 3, and 5, where all the temperatures meet at some certain loadings for each component. The fact that those two intersections appear in some figures and one intersection or none appear in others depends on the nature of the adsorbate−adsorbent/adsorbate−adsorbate interactions that contribute to the values of the virial coefficients. The presence of the intersection also depends on the loading range on which the estimations are calculated because this phenomenon can sometimes occur at high loadings that are excluded from these figures so as not to exceed the practical ranges of loading over which the adsorption isotherms were measured.

Multicomponent Isosteric Heats of Adsorption. The derived equations can also be used for predicting multicomponent isosteric heats of adsorption in a pre-

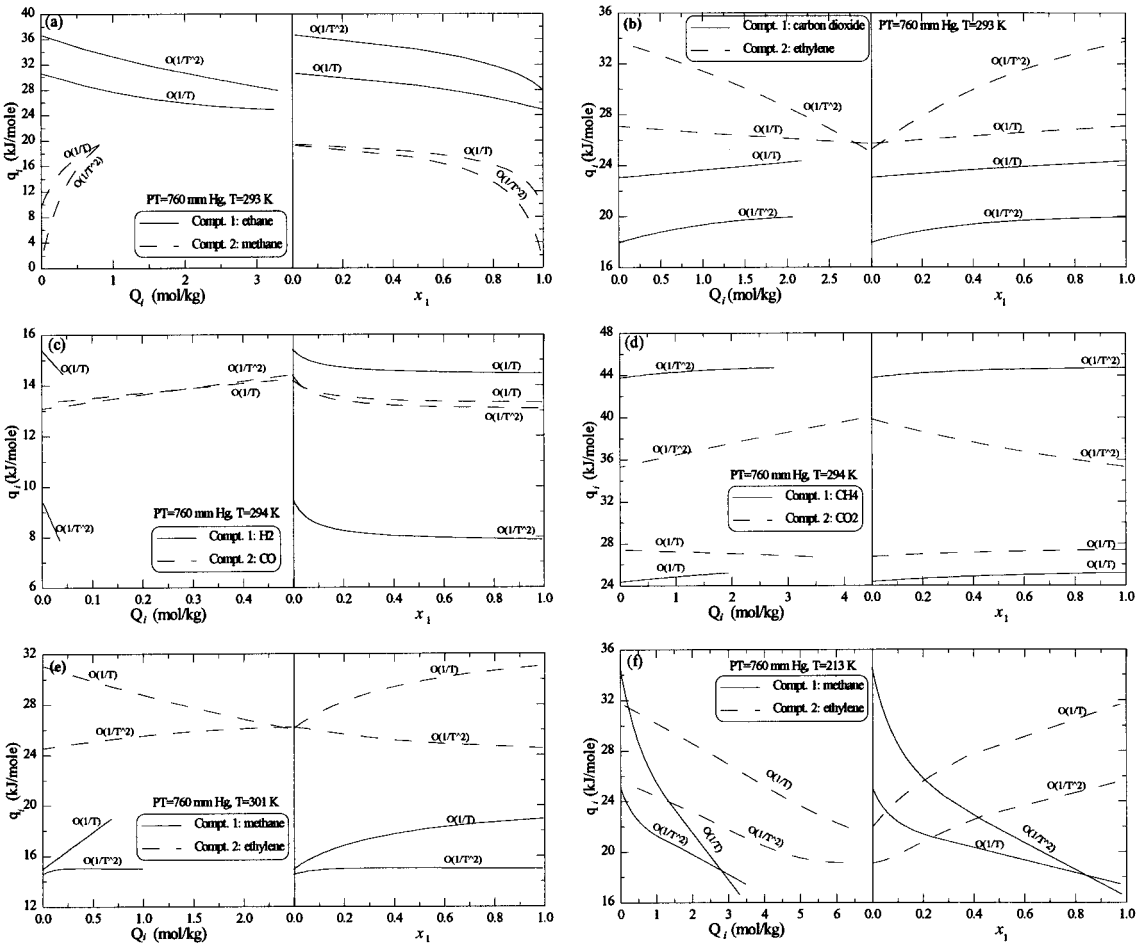

Figure 6. Sample binary isosteric heats of adsorption as a function of the amount adsorbed and the adsorbed phase composition on (a, b) Nuxite-AL-activated carbon (Szepesy and Illes, 1963c), (c, d) PCB-activated carbon (Ritter and Yang, 1987), and (e, f) BPL-activated carbon (Reich *et al.*, 1980) showing that the isosteric heats of adsorption predicted by $O(T^{-1})$ virial equation were close to those of $O(T^{-2})$ only for lightly adsorbed components.

dictive mode (i.e., without using any binary or multicomponent experimental data). Multicomponent isosteric heats of adsorption can be predicted simply from eq 11 with the single-component isotherm parameters and the component loadings predicted from eq 3. This ability adds a very useful tool for simulating multicomponent adsorption processes using information only from the single-component adsorption isotherms. Considering that there is no published information on estimating isosteric heats of adsorption for more than binary systems (Karavias and Myers, 1991; Sircar, 1991a; Sircar, 1992), this technique was successfully applied to binary systems, ternary systems, a quadratic system, and a five-component system. All of the results are shown in Figures 6−10, with Figures 6, 7, and 9 focusing on binary trends, and Figures 8 and 10 focusing on multicomponent trends.

When dealing with equally adsorbable components at moderate-to-high temperatures, the isosteric heat predictions by the two types of virial coefficients were close to each other. However, when predicting the isosteric heats of adsorption of mixtures with components of different adsorption affinities (e.g., heavy−light and polar−nonpolar component combinations or at low temperatures, a considerable difference was noticed between the predictions corresponding to the two types of virial coefficients. This difference was understood to be related to the increased interaction forces at conditions under which a strong adsorption occurs, releasing a high amount of energy (e.g., at low temperatures), and the considerable surface heterogeneity towards different components with different adsorption affinities. Hence, the virial equation with $O(T^{-2})$ coefficients was believed to be superior under these conditions because of its ability to consider the various interactions as noticed in the predictions of the single-component isosteric heats of adsorption. The total pressure of the system seemed to have a negligible effect on its heterogeneity as indicated by close predictions obtained from both types of virial coefficients with various total pressures.

Sample distributions of the isosteric heats of adsorption for some of the binary systems at a constant total pressure of 1 atm are shown in Figure 6, which indicates that the differences between the isosteric heats of adsorption predicted by two orders of temperature dependencies were similar for equally adsorbed components at moderate temperatures, such as those shown in Figures 6a, 6c, and 6e. In contrast, when estimating the binary isosteric heats of adsorption for components with different adsorption affinities, such as those shown in Figures 6b and 6d, the difference between the estimations obtained from the two orders of the virial coefficients significantly increased. The same behavior was noticed when estimating the binary isosteric heats of adsorption at low temperature, such as that shown in Figure 6f, when compared to the estimations of the same system at a higher temperature, such as that shown in Figure 6e. Therefore, at such conditions where

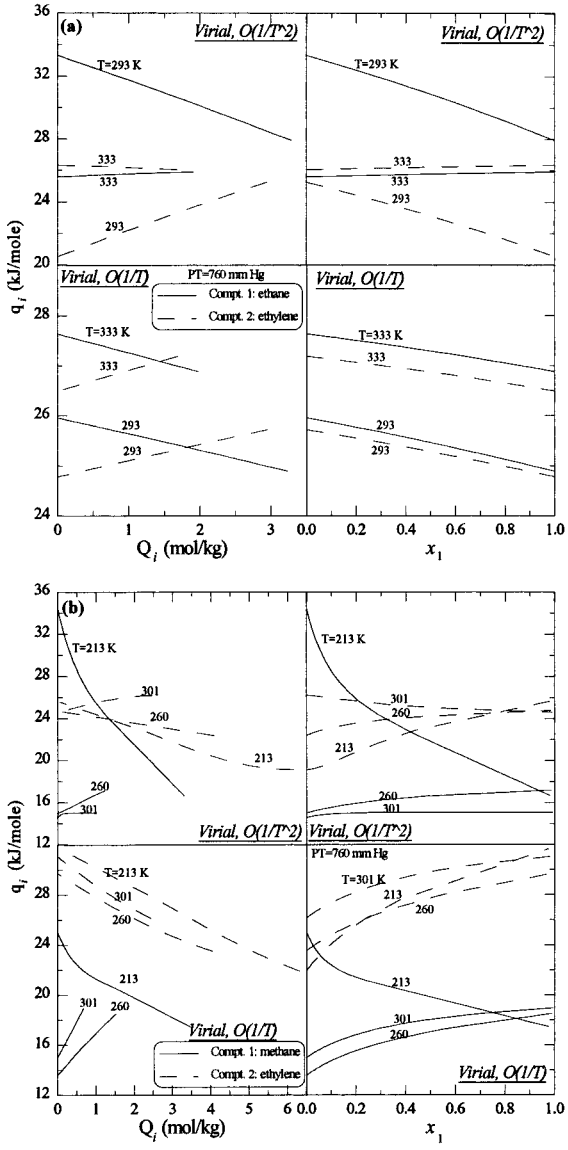

Figure 7. Sample temperature dependencies of the binary isosteric heats of adsorption as a function of the amount adsorbed and the adsorbed phase composition on (a) Nuxite-AL-activated carbon (Szepesy and Illes, 1963c), and (b) BPL-activated carbon (Reich *et al.*, 1980), showing that the isosteric heats of adsorption predicted by O(T^{-1}) virial equation were close to those of O(T^{-2}) only at moderate-to-relatively high temperatures.

a strong adsorption is expected or when a mixture of distinctly different adsorbates is considered, it is advisable to adopt the estimations with O(T^{-2}) virial coefficients or higher if large nonidealities or adsorption affinities are expected.

Figure 7 shows binary predictions calculated at a total pressure of 1 atm for equally adsorbed components at different temperatures. The predicted isosteric heats of adsorption were also noticed to be very close to each other for moderate-to-high temperatures. When considering low temperatures, however, the predictions tended to vary considerably from the others. This result was another indication of the increased interaction forces/heterogeneity observed at low temperatures. This difference was much more pronounced when using the virial equation with O(T^{-2}) coefficients. Moreover, the estimations obtained from the virial equation with O(T^{-1}) coefficients, such as those shown in the lower part of Figure 7b, can indicate misleading temperature

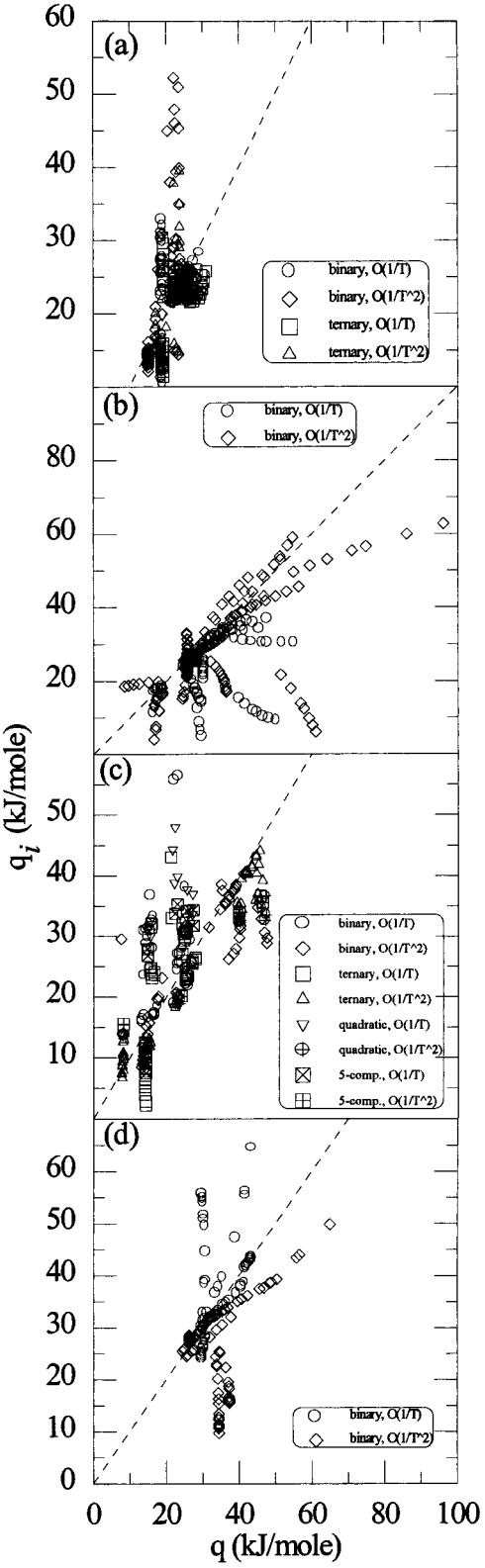

Figure 8. A comparison between single- and multicomponent isosteric heats of adsorption on (a) BPL-activated carbon (Reich *et al.*, 1980), (b) Nuxite-AL-activated carbon (Szepesy and Illes, 1963c), (c) PCB-activated carbon (Ritter and Yang, 1987), and (d) 13X molecular sieve zeolite (Danner and Choi, 1978; Hyun and Danner, 1982; Kaul, 1987), showing that the multicomponent isosteric heats of adsorption in some cases deviated significantly from the single-component isosteric heats of adsorption at the same partial loading (dotted lines indicate equality).

dependencies where the trend can be inverted with temperature. However, the estimations yielded from

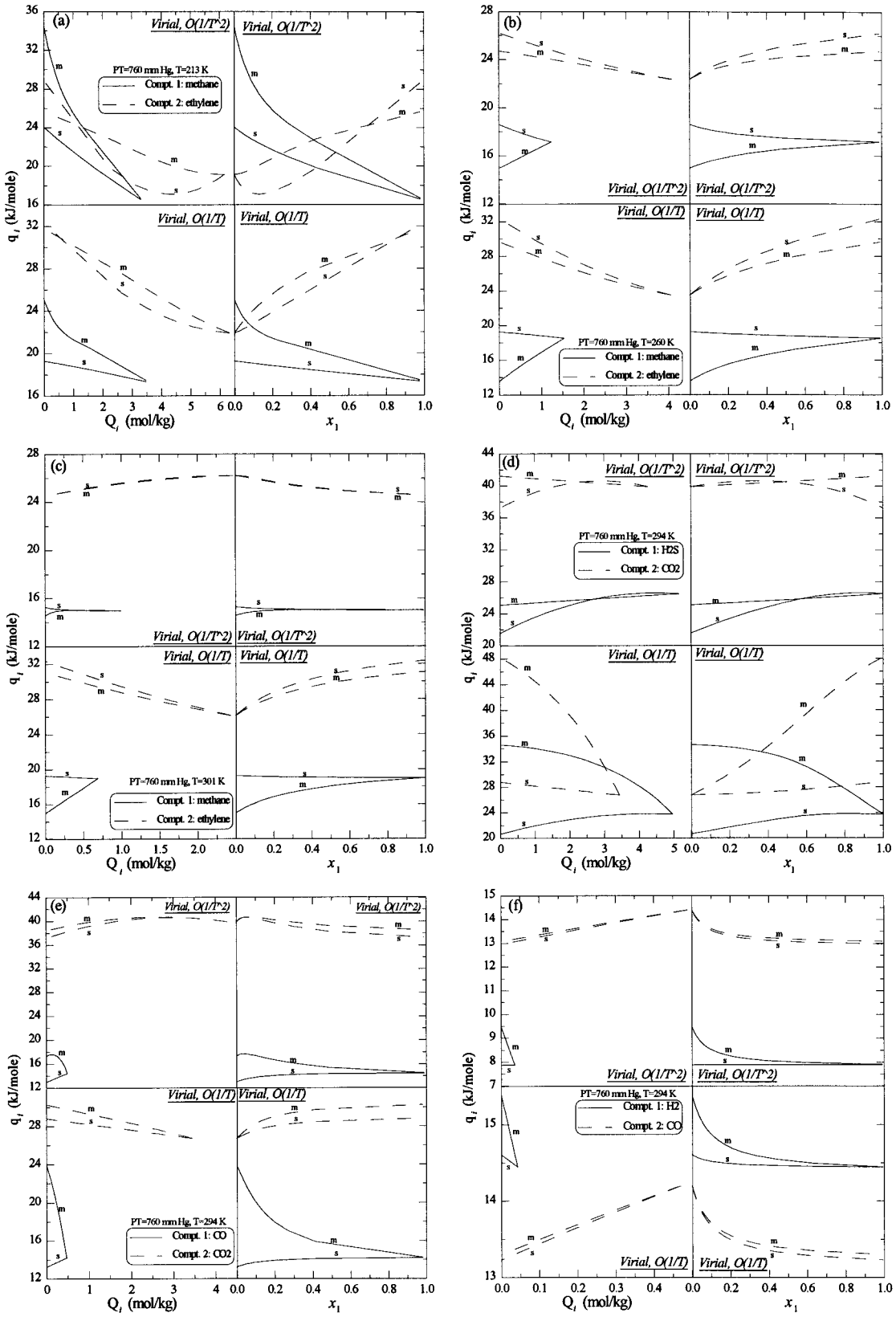

Figure 9. The difference between single- (s) and multicomponent (m) isosteric heats of adsorption as a function of the amount adsorbed and the adsorbed phase composition for both $O(T^{-1})$ and $O(T^{-2})$ on (a, b, c) BPL-activated (Reich *et al.*, 1980) and (d, e, f) PCB-activated carbon (Ritter and Yang, 1987), showing that the multicomponent isosteric heats of adsorption could not be approximated by the single-component isosteric heats of adsorption for low temperatures and/or heavily adsorbed components.

$O(T^{-2})$ coefficients, such as those shown in the upper part of Figure 7b, gave a very well-behaved temperature dependency. This is also understood to result from the fact that the single-component parameters, on which the multicomponent predictions are totally dependent, are more sensitive toward temperature variations when truncating eq 2 after the third term instead of the second term.

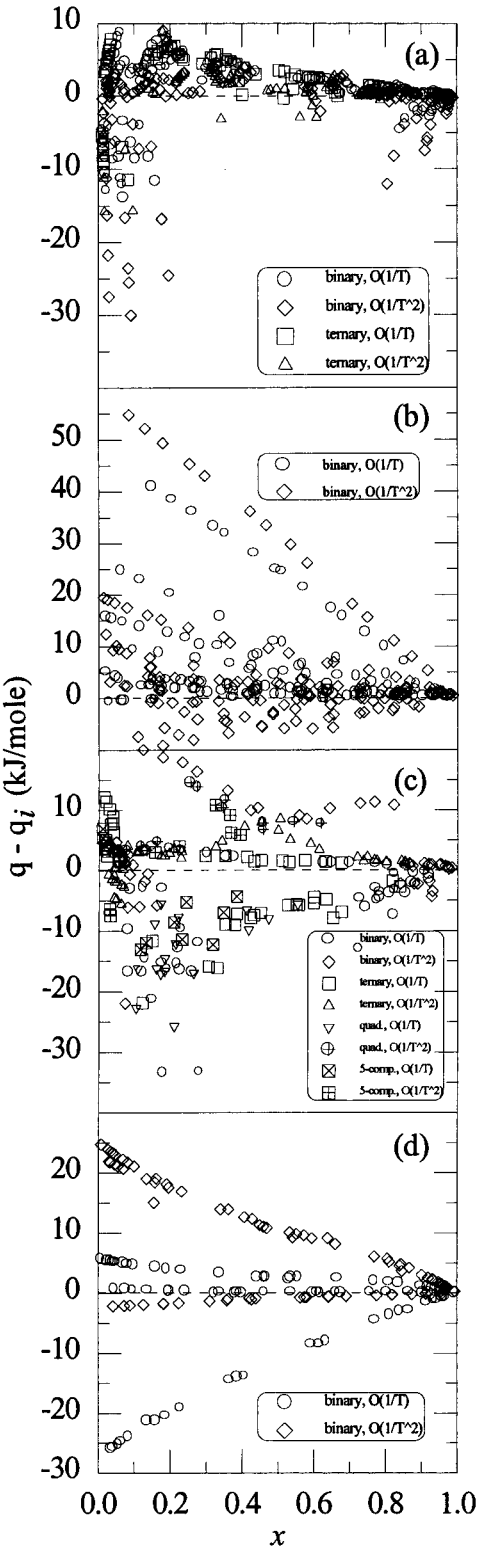

Figure 10. The difference between single- and multicomponent isosteric heats of adsorption as a function of the adsorbed phase composition on (a) BPL-activated carbon (Reich *et al.*, 1980), (b) Nuxite-AL-activated carbon (Szepesy and Illes, 1963c), (c) PCB-activated carbon (Ritter and Yang, 1987), and (d) 13X molecular sieve zeolite (Danner and Choi, 1978; Hyun and Danner, 1982; Kaul, 1987), showing that the difference increased significantly in the case of infinite dilution in the adsorbed phase (dotted lines indicate equality).

Figure 8 shows a comparison between the predicted single- and multicomponent isosteric heats of adsorption (calculated at the same temperature and partial loading for each point and type of virial coefficient) for several binary/multicomponent combinations on different adsorbents. It is clear from Figure 8 that there are some factors that can cause the multicomponent isosteric heats of adsorption to differ considerably from the single-component isosteric heats of adsorption. Such factors are shown by the clear trends at which the predictions deviated from the equality criterion (dotted lines), as those noticed in Figures 8a, 8b, and 8d.

Figure 9 shows comparisons between the estimations of some binary isosteric heats of adsorption (marked with "m") and the corresponding single-component isosteric heats of adsorption (marked with "s") calculated from the virial equation with the same order of temperature dependence at the same partial loading of each component. The binary isosteric heats of adsorption were close to the single-component isosteric heats of adsorption at the same partial loading only when using a temperature-sensitive method of prediction (such as the virial equation with $O(T^{-2})$ coefficients) with light adsorbates and at moderate-to-high temperatures. Therefore, the single-component estimations with $O(T^{-2})$ virial coefficients (the upper part of Figures 9a−9f) were much closer to the binary isosteric heats of adsorption than those with $O(T^{-1})$ virial coefficients (the lower part of Figures 9a−9f). The differences between the single and binary isosteric heats of adsorption also decreased considerably with increasing temperature. Examples of this phenomenon were the isosteric heats of adsorption of methane and ethylene on BPL-activated carbon at 213, 260, and 301 K shown in Figures 9a, 9b, and 9c, respectively. When comparing these differences at a fixed, moderate temperature for different adsorbate mixtures, such as those shown in Figures 9d, 9e, and 9f, the difference increases when heavier adsorbates were considered. Therefore, it is advisable to use the suggested multicomponent model rather than approximating the multicomponent isosteric heats of adsorption from the single-component isosteric heats of adsorption, for any order of estimations, whenever high adsorption affinity or nonideality are expected.

Figure 10 shows that large deviations between the single- and multicomponent isosteric heats of adsorption resulted when the adsorbed phase mole fraction of one of the components in the mixture was low (e.g., <25%). Under these circumstances the predicted multicomponent isosteric heats of adsorption were considerably different from the single-component ones at the same temperature and partial loading. This result suggests that multicomponent adsorption process models that typically utilized constant, single-component isosteric heats of adsorption (e.g., Doong and Yang, 1986; Kapoor and Yang, 1988; and Cen and Yang, 1985) may have severely over- and/or underpredicted the total heat load in the system, especially if nonisothermal effects were important in the simulations and if one or more of the adsorbed phase mole fractions of the components fell below ~25% anywhere within the column during the simulation. Clearly, experimental mixed-gas isosteric heats of adsorption are needed to verify this intriguing result.

Figures 9 and 10 also show the consistency of the proposed formulations for the multicomponent heats of adsorption, which always approached the single-component heats of adsorption as the mole fraction of a particular component approached unity. This consis-

tency was always observed regardless of the temperature dependency, conditions, or expected heterogeneity of the system.

Conclusions

A very useful tool for the prediction of the isosteric heat of adsorption of single- and multicomponent gas adsorption was derived with the virial adsorption isotherm. Explicit expressions were obtained in terms of single-component isotherm parameters, only. The new model of the isosteric heat of adsorption has the advantage of accounting for the temperature effect and being used for any number of components in mixed-gas adsorption in a purely predictive mode. The new model also indicates the conditions when lateral or vertical interactions dominate when using $O(T^{-2})$ virial coefficients. Overall, the new formula is expected to have more accurate predictions of the isosteric heat of adsorption of binary and multicomponent mixtures than the usual techniques that require a chain rule application followed by numerical differentiation. What remains to be done, however, is an extensive comparison with experimental binary and multicomponent isosteric heats of adsorption. This kind of data is nearly nonexistent in the literature because of the difficulties associated with its measurement.

Acknowledgment

The authors gratefully acknowledge financial support from the National Science Foundation under Grant CTS-9410630 and from the Westvaco Charleston Research Center.

Nomenclature

a = adsorbent specific surface area, m^2/kg
A = first virial coefficient, dimensionless
A' = temperature derivative of the first virial coefficient, K^{-1}
ARE = absolute relative error, %
B = second virial coefficient, $kg \cdot m^2/mol$ adsorbed
B' = temperature derivative of the second virial coefficient, $kg \cdot m^2/K \cdot mol$ adsorbed
C = third virial coefficient, $kg^2 \cdot m^4/mol^2$ adsorbed
C' = temperature derivative of the third virial coefficient, $kg^2 \cdot m^4/K \cdot mol^2$ adsorbed
m = counter
n = total number of data points
N = number of components in a gas mixture
$O(1/T)$ = corresponding to T^{-1} virial coefficients
$O(1/T^2)$ = corresponding to T^{-2} virial coefficients
P = absolute pressure, mmHg
P_i = partial pressure of component i, mmHg
q = single-component isosteric heat of adsorption, kJ/mol adsorbed
Q = adsorbed amount, mol/kg adsorbent
q_i = multicomponent isosteric heat of adsorption of component i, kJ/mol adsorbed
Q_i = partial amount adsorbed of component i, mol/kg adsorbent
q_i^o = isosteric heat of adsorption of pure component i, kJ/mol adsorbed
$q^{(1/T)}$ = single-component isosteric heat of adsorption with T^{-1} virial coefficients, kJ/mol adsorbed
$q^{(1/T^2)}$ = single-component isosteric heat of adsorption with T^{-2} virial coefficients, kJ/mol adsorbed
R = universal gas constant, kJ/mol·K
T = absolute temperature, K
x = adsorbed phase composition, mole fraction
y = fluid phase composition, mol fraction

Subscripts

exp = experimental
i = counter
j = counter
k = counter
opt = optimum, yielding a zero derivative
pred = predicted
Q = constant loading
T = constant temperature

Superscripts

calc = calculated data
exp = experimental data
(m) = T^{-m} virial coefficients, m = 0, 1, 2, ...
$(1/T)$ = corresponding to T^{-1} virial coefficients
$(1/T^2)$ = corresponding to T^{-2} virial coefficients

Literature Cited

Barrer, R. M.; Davies, J. A. Sorption in Decationated Zeolites I. Gases in Hydrogen Chabazite. *Proc. R. Soc. London* **1970**, *320*, 289.

Bering, B. P.; Serpinsky, V. V.; Surinova, S. I. Calculation of Adsorptional Equilibrium Parameters for Adsorbent-Binary Gas Systems. *Dokl. Akad. Nauk. SSSR* **1963**, *153*, 129.

Cen, P.; Yang, R. Separation of a Five-Component Gas Mixture by Pressure Swing Adsorption. *Sep. Sci. Technol.* **1985**, *20*, 725.

Czepiriski, L.; Jagiello, J. Virial-Type Thermal Equation of Gas-Solid Adsorption. *Chem. Eng. Sci.* **1989**, *44*, 797.

Danner, R. P.; Choi, E. C. Mixture Adsorption Equilibria of Ethane and Ethylene on 13X Molecular Sieves. *Ind. Eng. Chem. Fund.* **1978**, *17*, 248.

DeGance, A. E. Multicomponent High-Pressure Adsorption Equilibria on Carbon Substrates: Theory and Data. *Fluid Phase Equilib.* **1992**, *78*, 99.

DeGance, A. E.; Morgan, W. D.; Yee, D. High Pressure Adsorption of Methane, Nitrogen, and Carbon Dioxide on Coal Substrates. *Fluid Phase Equilib.* **1993**, *82*, 215.

Doong, S.; Yang, R. Bulk Separation of Multicomponent Gas Mixtures by Pressure Swing Adsorption: Pore/Surface Diffusion and Equilibrium Models. *AIChE J.* **1986**, *32*, 397.

Dubinin, M. M. Fundamentals of the Theory of Adsorption in Micropores of Carbon Adsorbents: Characterization of their Adsorption Properties and Microporous Structures. *Carbon* **1989**, *27*, 457.

Dunne, J. A.; Mariwala, R.; Rao, M.; Sircar, S.; Gorte, R. J.; Myers, A. L. Calorimetric Heats of Adsorption and Adsorption Isotherms. 1.O_2, N_2, Ar, CO_2, CH_4, C_2H_6, and SF_6 on Silicate. *Langmuir* **1996a**, *12*, 5888.

Dunne, J. A.; Rao, M.; Sircar, S.; Gorte, R. J.; Myers, A. L. Calorimetric Heats of Adsorption and Adsorption Isotherms. 2. O_2, N_2, Ar, CO_2, CH_4, C_2H_6, and SF_6 on NaX, H-ZSM-5, and Na-ZSM-5 Zeolites. *Langmuir.* **1996b**, *12*, 5896.

Dunne, J. A.; Rao, M.; Sircar, S.; Gorte, R. J.; Myers, A. L. Calorimetric Heats of Adsorption and Adsorption Isotherms. 3. Mixtures of CH_4 and C_2H_6 in Salicalite and Mixtures of CO_2 and C_2H_6 in NaX. *Langmuir* **1997**, *13*, 4333.

Hacskaylo, J. J.; LeVan, M. D. Correlation of Adsorption Equilibrium Data Using a Modified Antoine Equation: A New Approach for Pore-Filling Models. *Langmuir* **1985**, *1*, 97.

Handy, B. E.; Sharma, S. B.; Spiewak, B. E.; Dumesic, J. A. A Tian-Calvet Heat-Flux Microcalorimeter for Measurement of Differential Heats of Adsorption. *Meas. Sci. Technol.* **1993**, *4*, 1350.

Haydel, J. J.; Kobayashi, R. Adsorption Equilibria in the Methane-Propane-Silica Gel System at High Pressures. *Ind. Eng. Chem. Fund.* **1967**, *6*, 546.

Hyun, S. H.; Danner, R. P. Equilibrium Adsorption of Ethane, Ethylene, Isobutane, Carbon Dioxide, and Their Binary Mixtures on 13X Molecular Sieves. *J. Chem. Eng. Data* **1982**, *27*, 196.

Kapoor, A.; Yang, R. Separation of Hydrogen-Lean Mixtures for a High-Purity Hydrogen by Vacuum Swing Adsorption. *Sep. Sci. Technol.* **1988**, *23*, 153.

Kapoor, A.; Ritter, J. A.; Yang, R. T. An Extended Langmuir Model for Adsorption of Gas Mixtures on Heterogeneous Surfaces. *Langmuir* **1990**, *6*, 660.

Karavias, F.; Myers, A. Isosteric Heats of Multicomponent Adsorption: Thermodynamics and Computer Simulations. *Langmuir* **1991**, *7*, 3118.

Kaul, B. K. Modern Version of Volumetric Apparatus for Measuring Gas-Solid Equilibrium Data. *Ind. Eng. Chem. Res.* **1987**, *26*, 928.

O'Neil, M.; Louvrien, R.; Phillips, J. New Microcalorimeter for the Measurement of Differential Heats of Adsorption of Gases on High Surface Area Solids. *Rev. Sci. Instrum.* **1985**, *56*, 2312.

Pan, H.; Ritter, J. A.; Balbuena, P. B. Isosteric Heats of Adsorption on Carbon Predicted by Denisty Functional Theory. *Ind. Eng. Chem. Res.* **1998**, in press.

Parillo, D. J.; Gorte, R. J. Characterization of Stoichiometric Adsorption Complexes in H-ZSM-5 Using Microcalorimetry. *Catal. Lett.* **1992**, *16*, 17.

Pierotti, R.; Thomas, H. Virial Analysis of Low-Coverage Physical Adsorption Data on Heterogeneous Surfaces. *J. Chem. Soc. Faraday Trans. 1* **1974**, *70*, 1725.

Polanyi, M. Theories of the Adsorption of Gases. A General Survey and some Additional Remarks. *Trans. Faraday Soc.* **1932**, *28*, 316.

Reich, R.; Ziegler, W. T.; Rogers, K. A. Adsorption of Methane, Ethane, and Ethylene Gases and Their Binary and Ternary Mixtures and Carbon Dioxide on Activated Carbon at 212−301 K and Pressures to 35 Atmospheres. *Ind. Eng. Chem. Process Des. Dev.* **1980**, *19*, 336.

Ritter, J. A.; Yang, R. T. Equilibrium Adsorption of Multicomponent Gas Mixtures at Elevated Pressures. *Ind. Eng. Chem. Res.* **1987**, *26*, 1679.

Sircar, S. Isosteric Heats of Multicomponent Gas Adsorption on Heterogeneous Adsorbents. *Langmuir* **1991a**, *7*, 3065.

Sircar, S. Role of Adsorbent Heterogeneity on Mixed Gas Adsorption. *Ind. Eng. Chem. Res.* **1991b**, *30*, 1032.

Sircar, S. Estimation of Isosteric Heats of Adsorption of Single Gas and Multicomponent Gas Mixtures. *Ind. Eng. Chem. Res.* **1992**, *31*, 1813 .

Szepesy, L.; Illes, V. Adsorption of Gases and Gas Mixtures, I. Measurement of the Adsorption Isotherms of Gases on Active Carbon up to Pressures of 1000 torr. *Acta Chim. Hung. Tomus* **1963a**, *35*, 37.

Szepesy, L.; Illes, V. Adsorption of Gases and Gas Mixtures, II. Measurement of the Adsorption Isotherms of Gases on Active Carbon Under Pressures of 1 to 7 ATM. *Acta Chim. Hung. Tomus* **1963b**, *35*, 53.

Szepesy, L.; Illes, V. Adsorption of Gases and Gas Mixtures, III. Investigation of the Adsorption Equilibria of Binary Gas Mixtures. *Acta Chim. Hung. Tomus* **1963c**, *35*, 245.

Taqvi, S. M.; LeVan, M. D. A Simple Way to Describe Nonisothermal Adsorption Equilibrium Data Using Polynomials Orthogonal to Summation. *Ind. Eng. Chem. Res.* **1997a**, *36*, 419.

Taqvi, S. M.; LeVan, M. D. Virial Description of Two-Component Adsorption on Homogeneous and Heterogeneous Surfaces. *Ind. Eng. Chem. Res.* **1997b**, *36*, 2197.

Valenzuela, D. P.; Myers, A. L. *Adsorption Equilibrium Data Handbook*; Prentice Hall: Englewood Cliffs, NJ, 1989.

Zhang, S. Y.; Talu, O.; Hayhurst, D. T. High Pressure Adsorption of Methane in NaX, MgX, CaX, SrX, and BaX. *J. Phys. Chem.* **1991,** *95*, 1722.

Received for review August 22, 1997
Revised manuscript received October 3, 1997
Accepted October 30, 1997

IE970577Y